IET Intelligent Transport Systems

WILEY

The Institution of Engineering and Technology

CASE STUDY OPEN ACCESS

Understanding Urban Mobility Responses to Extreme Precipitation Events: A Case Study of Zhengzhou, China

Qian Ye[1] | Yulin Ma[2] | Shucai Xu[3] | Miguel Ángel Sotelo[4] | Zhixiong Li[5]

[1]Transport Planning and Research Institute Ministry of Transport, Beijing, China | [2]School of Mechanical and Automotive Engineering, Anhui Polytechnic University, Wuhu, China | [3]National Key Laboratory of Intelligent Green Vehicles and Transportation, Tsinghua University, Beijing, China | [4]Department of Computer Engineering, University of Alcala, Madrid, Spain | [5]Faculty of Mechniacal Engineering, Opole University of Technology, Opole, Poland

Correspondence: Yulin Ma (mayulin@mail.ahpu.edu.cn) | Zhixiong Li (zhixiong.li@yonsei.ac.kr)

Received: 13 June 2023 | **Revised:** 25 February 2024 | **Accepted:** 2 May 2025

Funding: This work was supported in part by the Natural Science Research Project of Anhui Educational Committee under Grant No. 2023AH020015; and in part by the Applied Basic Research Project of Wuhu under Grant No. 2023jc10.

ABSTRACT

Cities are increasingly vulnerable to the impacts of extreme weather events, understanding the travel responses to such events can support needs-based emergency resource allocation and long-term resilience planning. Although previous research has advanced our understanding of travel patterns during abnormal conditions, knowledge remains limited regarding how urban travel changes spatially (e.g. by different spatial clusters) during extreme precipitation events. To address this research gap, this study aims to assesses how urban travel, by number of trips, changed in response to extreme precipitation events using time series clustering and discrete choice modelling. The study uses cell phone signalling-based mobility big data before, during, and after the perturbations, with the 2021 Zhengzhou floods as a case study. Moreover, the aggregated responses of urban travel were empirically defined in terms of the magnitude of trip reduction and time-to-recovery, i.e. travel resilience. The study identifies four distinct groups that exhibit comparable response and recovery patterns, which can be subject to the influence of factors associated with the built environment. The study reveals that areas with higher road network density are comparatively more vulnerable to the initial impact of extreme rainfall and flooding. Nevertheless, taking a long-term perspective, higher road network density contributes to faster recovery and more robust travel resilience. Moreover, home-based work trips are less sensitive to red rainfall warnings than home-based other trips and non-home-based trips. This study provides valuable implications for planners and policymakers to resist similar future events.

1 | Introduction

Cities worldwide have witnessed a rising number of extreme weather events (EWEs) in the past decades due to anthropogenic climate changes. These EWEs often result in various hazards such as heavy rainfall and pluvial flooding, which can cause significant damage to transportation infrastructure [1, 2]. Moreover, they can have severe impacts on people's daily lives, including travel disruptions and even loss of life. A recent example of this occurred on July 20th, 2021, when Zhengzhou, China was hit by extreme precipitation, leading to massive traffic network disruption and accidents. The flooding of metro line 5 resulted in the tragic loss of 14 lives, and another six people lost their lives on the Jing-guang Expressway. Studies in the transportation field have shown that changes in travel behaviour as a response to EWEs can either mitigate or exacerbate the impact of climate hazards [2]. For instance, it has been found that walking or driving into floodwaters is the primary cause of road drowning during flooding events [3]. Therefore, to develop effective emergency management measures, it is crucial to consider the disaster characteristics from various information sources and the travel responses during and after hazardous conditions.

Understanding the travel responses of citizens during climate hazards, such as extreme precipitation, is crucial for effective urban disaster preparedness and relief operations. This information can help assess the effectiveness and variability of local travel response and support community recovery trends [4], which, in turn, can aid in needs-based resource allocation and long-term planning strategies [2, 4]. It is important to note that if human flows in a given space-time are less focused during the pre-disaster period, especially when weather forecasts are limited by spatial and temporal scales, it may lead to massive deaths and economic losses. In the transportation research community, travel patterns have been shown to follow specific laws in normal conditions, such as the power-law distribution [1]. However, citizens are less likely to travel or move in hazardous conditions as they would in normal periods, or even more complex. This is because bounded rationality [5], shaped by a range of socio-economic determinants such as socio-demographics, life circumstances, attitudes, and personalities, leads to different cognitive limits and response behaviours [5, 6]. Additionally, people living in different regions of the city can be affected by different infrastructure failures and service disruptions [7, 8]. Thus, the outcome of a disaster is not only related to the severity of the disaster but also to the human flows of spatial-temporal heterogeneity, where travel responses play a pivotal role.

Although many studies have attempted to examine travel behaviours during disaster scenarios, there is limited research on how urban travel changes spatially, such as by different spatial clusters, under extreme precipitation events. In the field of transportation, travel behaviour under abnormal conditions is a popular research topic, with scenarios including natural disasters [9, 10], technological system failures [11, 12], public health events [13, 14], and meteorological events [15–17]. For example, Golshani et al. [10] studied the evacuation demand model-tour formation behaviour during no-notice emergency events, and Abad et al. [9] analysed the adaptations of commuting behaviour of transit users in Metro Manila to flooding. However, there are several shortcomings in current research: Firstly, traditional survey-based behavioural research is time-consuming and labour-intensive, with limited geographical areas, and fails to enable near-real-time dynamic tracking [4]. The proliferation of location-based mobility data in recent years offers additional opportunities with the help of computerized algorithms [1, 4]. However, empirical analysis for extreme precipitation scenarios is still lacking as constrained by data limitations. Secondly, the role of built environment characteristics in response and recovery from extreme precipitation remains unknown, which may hinder the allocation of emergency resources and the prioritization of resilience planning measures. Last but not least, the response of different trip types (home-based work, HBW; home-based other, HBO; non-home-based, NHB) to red rainfall warnings[1] or weather forecasts has not been explored empirically in existing studies. This information is crucial for developing targeted intervention strategies and emergency response plans that can effectively mitigate the impact of extreme precipitation events.

To address the aforementioned research gap, this study aims to assess how urban travel, by number of trips, changes in response to extreme precipitation events under different geographical contexts, based on time series clustering and discrete choice modelling. As a case study, the "7–20" extreme rainfall and flooding event in Zhengzhou city, China in 2021 will be examined. The empirical analysis process consists of three modules. Firstly, the study characterizes the travel response of citizens under extreme precipitation. Specifically, the response patterns of different geographical grids (1000 m $\times$ 1000 m) are characterized using the time series clustering algorithm K-SHAPE [18], with the total number of trips attracted and generated as input. Secondly, the study defines the response patterns in terms of resilience, and analyses the role of built environment factors in the heterogeneity of responses, including trip reduction and time-to-recovery, using multinomial logit (MNL) models. Lastly, the study investigates the responses of different trip types to the red rainfall warning. The results of this study are expected to contribute to the existing body of knowledge on mobility disturbances caused by extreme precipitation events and provide new insights for urban policy-makers and emergency responders to make more informed decisions to increase the climate resilience of cities. Furthermore, this research contributes to the field of geospatial big data analysis for resilient cities in the following ways:

1. Firstly, it explores travel response patterns under extreme precipitation and its derivative hazards, such as flooding, in association with built environment factors. This information can assist in needs-based resource allocation and the development of long-term transportation resilience planning strategies.
2. Secondly, the analysis of the responses of different trip types to red rainfall warnings provides a basis for emergency preparedness. For instance, this analysis can help prioritize the allocation of risk management measures for areas where trips are concentrated but less sensitive to warnings.
3. Lastly, the analytical framework developed in this study based on mobile phone signalling data can be used for empirical analysis of other extreme or unexpected events, beyond natural disasters.

The remainder of the paper is organized as follows. Section 2 identifies research gaps through a comprehensive review of the relevant literature. Sections 3 and 4 present the data and methodology respectively. Section 5 discusses the results of the analysis, while Section 6 concludes and summarizes.

2 | Literature Review

2.1 | Travel Decision-Making Behaviour During Abnormal Conditions

Recent research has made significant strides in advancing our understanding of travel decision-making behaviour, especially with respect to evacuation behaviour during abnormal conditions in cities. This is because cities have experienced an increasing number of disruptions from various types of unexpected events. Existing studies on travel behaviour can be categorized into two decision-making periods: pre-trip and en-route. For instance, Hamilton et al. [19] analysed electronic interventions based on the implementation of images to alter driving behaviour during flooding. Tang et al. [20] estimated the alighting stops of bus trips from open smart card data by incorporating weather conditions and travel history. These decisions made during travel include travel (evacuation) or not, destination choice, mode choice, departure time choice, and route selection. Most studies have focused on home-based travel decision and mode choice. In general, research scenarios include natural disasters, production incidents, public health events, and climate events. For example, hurricanes [21, 22], typhoons [23], wildfires [24], volcanic eruptions [25], earthquakes [26], tsunamis (Buylova et al., 2020), and flooding [9, 27] are the main natural disaster scenarios being studied. Technological system failures focus on building fires [11] and chemical leakage accidents [28]. Contagious respiratory illnesses are the main subject of studies related to public health events, with the COVID-19 pandemic being the most studied. Moreover, current research has also addressed changes in travel behaviour under the impact of climate hazards, with analyses carried out at high/low temperatures [16, 29], rainfall [15, 30, 31], wind speed [31] etc., covering both short term or immediate and seasonal long-term impacts. For example, Mirzaei et al. [29] studied the effects of the built environment, weather conditions, and travel departure time on mode choice decisions for different travel purposes, using Isfahan, Iran, as a case study.

The theory of travel decision-making primarily applies normative decision theory. Normative decision theory is the focus of research in decision theory or choice analysis and refers to the prerequisites of rational decision making [32]. It revolves around the idea of what the decision-maker "should do" based on the abstraction of assumptions about one's self-interest in decision-making behaviour [32, 33]. In general, experimental design and choice experiments, discrete choice models and statistical inference form the basis of normative research [34]. The factors involved in travel decision-making in normative research include personal knowledge and experience, socio-economic characteristics, and the decision-making environment, including built environment characteristics, hazard characteristics, weather, and government measures. Typical analytical models include optimization theory, logistic regression, and its extensions, structural equation models, and geographically weighted regression models. For example, Abad et al. [9] applied a series of binary logistic models and revealed that perceived flood characteristics, socio-demographic conditions, and commuters' beliefs about the frequency of flood events over time all played a role in the adaptation of commuting behaviour by transit users. In their study of meteorological effects using a regression model, Liu et al. [15] found that a 1 mm increase in precipitation was associated with a 0.39% increase in the number of ride-hailing services and a 1 m/s increase in wind speed would result in a 1.04% decrease in ride-hailing demand.

However, some studies have suggested that the assumption of "Homo Economicus" is unrealistic and fails to account for a variety of paradoxes that are inconsistent with actual behaviours [33]. "Homo Economicus" characterizes humans as being selfish, rational maximizers of personal utility as defined in classical economics (e.g. [35]). For example, the Allais paradox and the Ellsberg paradox demonstrate that individuals often make choices that do not adhere to the rationality assumptions of "Homo Economicus." In the Allais paradox, individuals often exhibit loss aversion by choosing the option with a lower expected utility but a higher probability of avoiding losses, even in high-risk situations. This behaviour is inconsistent with the expected utility theory, which assumes that people always choose the option that maximizes their expected utility [6]. Prospect theory also gives an improvement on maximizing expected utility over reality. It suggests that when faced with a risky choice leading to gains agents are risk averse, preferring the certain outcome with a lower expected utility. However, when faced with a risky choice leading to losses agents are risk seeking, preferring the outcome that has a lower expected utility but the potential to avoid losses [6]. As a result, behavioural economics has garnered significant attention in travel decision-making research under abnormal conditions. Prospect theory, a descriptive, empirically valid model of choice, and its extensions are the most widely used, followed by regret theory and its extensions. For example, [36] developed a prospect theory-based framework to model the evolution of travellers' route choice under risk. Additionally, the random regret minimization model has been applied in evacuation studies using hypothetical stated preference data [12, 37]; Wong et al. [12] conducted a revealed preference survey for wildfire evacuation to assess the applicability of regret minimization to actual evacuation behaviour.

2.2 | Location-Based Services (LBS) Data in Travel Behaviour Under Unexpected Events

In recent times, the utilization of location-based services (LBS) data has seen extensive application in empirically investigating travel behaviour within the context of unforeseen events. The salient advantage of LBS data lies in its capacity to facilitate rapid response analyses, particularly pertinent when dealing with time-sensitive emergency situations, as highlighted in studies by Chen et al. [1] and Hong et al. [4]. The array of data sources encompasses mobile phone cellular signalling data, social media check-in data, and internet-based app location service data. To exemplify, Zhou et al. [38] harnessed automated fare collection (AFC) data to scrutinize the spatiotemporal ramifications of extreme rainfall events on metro ridership characteristics. Furthermore, mobility, serving as a metric to gauge the spatiotemporal movement of individuals or populations, has evolved into a fundamental proxy for assessing travel responses. The scrutiny of mobility disruptions within transportation infrastructure provides crucial insights into the adaptability of said infrastructure in the face of extreme events. Consequently, the examination of human mobility perturbations, leveraging metrics such as displacement, travel flows, and origin-destination (OD) pairs, has emerged as an innovative and potent methodology for evaluating the resilience of transportation infrastructure. Notably, Zhang and Li [8] leveraged anonymized mobile phone geolocation records to characterize individual mobility perturbations during extreme weather events in urban settings. Research inquiries related to mobility encompass a spectrum of vital aspects, including the impact of unforeseen events on human mobility, forecasts of mobility perturbations, determinants influencing mobility behaviour, prognosis of evacuation destinations, and the quantification of human mobility resilience, as elucidated by Wang et al. [39]. Furthermore, studies by Hong et al. (2020)

and Zhang et al. [40] conducted a granular analysis of mobility patterns during disaster events, exemplified by Hurricane Harvey in Houston and extreme weather occurrences in Nanjing, respectively. These investigations operationalized the concept of community resilience by scrutinizing alterations in mobility behaviour both pre-, during, and post-disasters, thereby facilitating the quantitative assessment of the magnitude of impact and the temporal dimensions of recovery. In parallel, the research conducted by Chen et al. [1] delved into the repercussions of extreme weather events on disruptions in urban pedestrian flow, with particular emphasis on the context of Typhoon Mangkhut's impact in Shenzhen, China, employing location-based service data. Simultaneously, geotagged Twitter data has found widespread adoption as a valuable resource for examining the influence of hurricanes on human mobility, exemplified by studies from Ahmouda et al. [41] and Wang et al. [39]. Collectively, these studies harness location-based data to unearth invaluable insights into the characteristics of mobility disturbances, offering practical guidance to urban planners and policymakers in their endeavours to enhance urban disaster resilience. Importantly, our research makes a valuable contribution to the existing literature by focusing its analytical lens on the unique context of heavy rainfall scenarios, thereby enriching the collective knowledge in this domain.

2.3 | Brief Summary

Despite the increasing number of studies attempting to understand travel response behaviour in disaster situations, the understanding of how urban travel changes spatially, such as by different spatial clusters, under extreme precipitation events remains limited and fragmented. Furthermore, the factors that affect the disparities in urban travel responses at the grid level are still unclear. Most existing studies also focus solely on home-based trips, leaving the responses of different trip types to red rainfall warnings unexplored. This study aims to fill these research gaps by addressing the following research questions: How does urban travel, measured by the number of trips, respond to extreme precipitation events and their derived hazards across different geographical contexts? What factors mediate the various urban travel responses in terms of travel reduction and recovery? Lastly, how do different trip types respond to multiple red rainfall warnings?

3 | Data and Study Area

3.1 | Study Area

The present study focuses on the central district of Zhengzhou, encompassing Zhongyuan District, Erqi District, Jinshui District, Guancheng District, and Huiji District. Figure 1 illustrates the digital elevation model (DEM) of Zhengzhou city. The topography of Zhengzhou slopes from southwest to northeast, and the region experiences a subtropical monsoon climate characterized by hot and rainy summers. Furthermore, more than 100 urban rivers and flood channels from the Yellow and Huai River systems traverse the urban area, exacerbating the effects of concrete pavements and the urban heat island phenomenon. Consequently, the city faces varying degrees of heavy rainfall and internal flooding almost every year. Notably, between 2011 and 2018, 38 flooding incidents occurred, with 26 of them causing widespread impacts, primarily triggered by short-term precipitation, as per statistical data [42].

Zhengzhou, the capital of Henan Province, is a significant political, economic, technological, and educational centre of the province, as well as a major transportation hub for Central China. The central area of the city spans 891 square kilometres and is home to approximately 5.03 million residents, according to the 2021 bulletin of the Zhengzhou Municipal Bureau of Statistics (available at: https://tjj.zhengzhou.gov.cn/tjgb/index.jhtml). Moreover, the urban centre boasts a well-established public transportation system and a high-density road network [43]. On July 19–21, 2021, the study area was severely affected by flooding caused by heavy rainfall. The city's advanced public transportation system, dense population, road network, and river distribution make it an appropriate case for analysing community travel resilience.

3.2 | 2021 Zhengzhou Floods

Between 17–23 July 2021, Henan Province in China experienced unprecedented heavy rainfall and flooding. The deluge travelled from the west and passed over Zhengzhou City, resulting in severe waterlogging due to the city's terrain, which slopes from southwest to northeast. The downpour began on 19 July 2021 in Zhengzhou, and between 14:00 on 19 July and 14:00 on 20 July, the average precipitation in the city reached a staggering 253 mm. On 20 July alone, the average precipitation also peaked at 253 mm, with the hourly precipitation hitting an all-time high of 201.9 mm between 16:00 and 17:00, breaking the record for maximum hourly precipitation since measurements began in 1951. Despite the Zhengzhou Meteorological Bureau issuing six consecutive red rainfall warnings to the public via multimedia channels at 6:02 am, 9:08 am, 11:50 am, 13:25 pm, 16:01 pm, and 21:32 pm on 20 July 2021, the heavy rainfall still left 398 people dead or missing. The flooding also caused extensive damage to numerous underground spaces, including tunnels, metro stations, underground shopping malls, and car parks, resulting in the destruction of hundreds of thousands of cars.

The occurrence of extreme precipitation had devastating consequences, causing significant disruption to urban travel and activities. According to reports, more than 200 flights at Zhengzhou Airport were either cancelled or delayed, leading to the breakdown of some high-speed rail lines passing through the Zhengzhou area, leaving many passengers stranded. The central districts were hit the hardest, with metro stations and tunnels being submerged, including the Zhengzhou Metro Line 5, where 14 people lost their lives due to the flooding. Bridges and underpass tunnels were also affected, with the Jing-guang north expressway tunnel being one of the worst hit locations, resulting in the loss of six lives. Road surfaces were also reported to have collapsed, causing further damage. Furthermore, the flooding had a severe impact on the electricity and water supply systems. A total of 1194 communities lost electricity, while 1864 communities lost water during the disaster, causing widespread disruption and inconvenience to the affected residents.

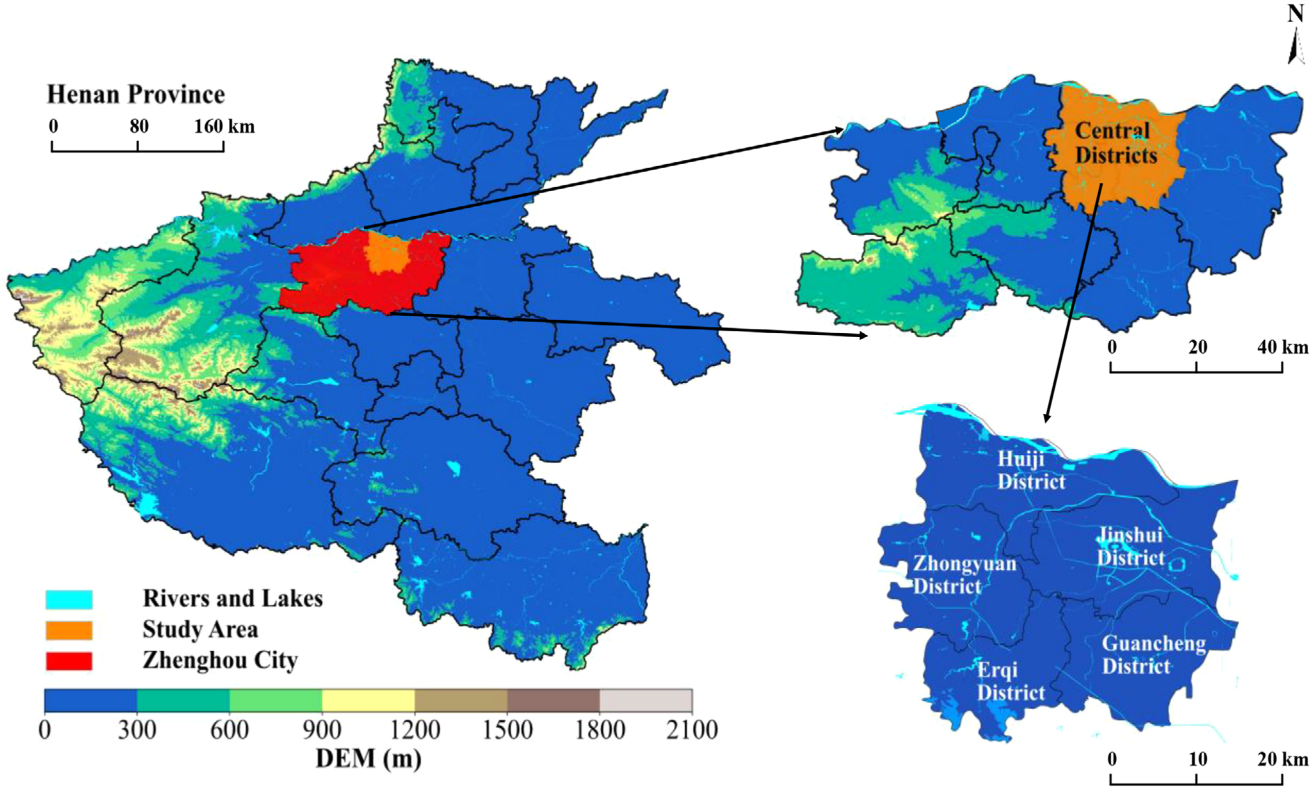

FIGURE 1 | Map of study area.

3.3 | Data

To comprehensively assess the spatiotemporal responses of urban travel during and after rainfall, five types of data were adopted:

3.3.1 | Aggregated and Anonymized Trip Data

The analysis was conducted using mobile phone cellular signalling data. To obtain aggregated origin-destination trip data, individual activity locations were first extracted based on specific rules. The initial home location was determined by selecting the geometric centre of the measurements with the longest and most frequent connections between 21:00 pm and 8:00 am on multiple days. Similarly, the initial work location (excluding the home location) was determined by selecting the geometric centre of the cell with the longest and most frequent connections between 9:00 am and 5:00 pm on weekdays. Locations with a dwell time of more than 30 min were considered secondary activity locations. However, the same activity location may appear different in coordinates due to oscillations. To address this, if the activity was interfered with neighbouring cells, the multiple sets of locations were further weighted by frequency and chosen as the final location. Moreover, the study area was divided into small grids to derive the aggregated origin-destination trip matrix.

The reliability and representativeness of the aggregated trip data were thoroughly examined. The data covered a period of 21 days from 12 to 31 July 2021, which included the 7 days before the disaster event (7.12–7.18), the 7 days during the event (7.19–7.25), and the 6 days after the event (7.26–7.31). In the data cleaning process, trips with travel distances less than 500 meters or travel times less than 5 min were excluded. The reason for this choice is based on existing literature related to mobile phone mobile data cleaning; for example, Wang et al., [44] believe that 5-min threshold follows the rule used in many household travel surveys to define what counts for an activity [45] and is also used as an appropriate threshold for an activity location in activity-based modelling [46]. Wang et al., [44] also believe that 200 m threshold, so that a displacement of 200 m in 5 min is equivalent to half the average walking speed (0.7 m/s). However, there are many modes to travel within the city, and the 200-meter threshold may be too low. In this regard, we refer to the research of Alexander et al., [47] and set the distance threshold to 500 meters. Comparison with reports on commuting characteristics released by Chinese map operators Baidu Maps (similar to Google Maps) in 2021 shows that such a threshold is feasible.

As a result, the average daily numbers of home-based work trips and home-based other trips were 0.499 million and 1.007 million, respectively, during the study period, compared to 0.78 million for non-home-based trips. Furthermore, the descriptive statistics revealed that the average daily commuting distance during the study period was close to the 8.9 km reported by Baidu Maps (similar to Google Maps) in 2021, as illustrated in Figure 2a. Due to the issues such as strict privacy and legal considerations, limited mobility and autonomy and data accuracy and reliability, the groups younger than 14 years old is excluded in the analysis. The analysis showed a tendency towards individuals aged between 15 and 59 years old, with a male bias compared to the seventh census in Zhengzhou, as demonstrated in Figure 2b,c. Similar

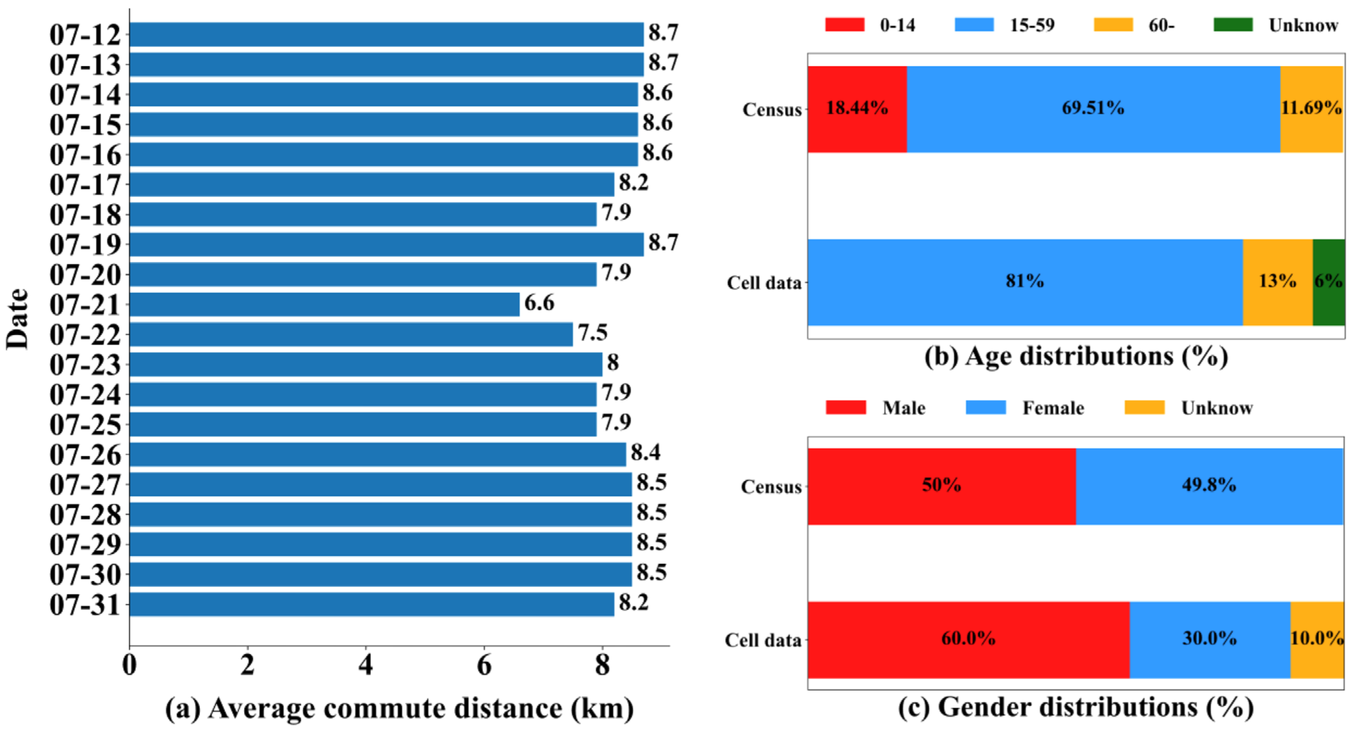

FIGURE 2 | Descriptive analysis of aggregated data.

observations were also reported in related studies such as Zhang and Li [8].

3.3.2 | Point-of-Interest (POI) Data

The study obtained over one million points of interest (POI) data from Baidu Maps for the study area. Each data point included information such as coordinates, name, and address. The POIs were classified into seven distinct categories, including administrative agencies, companies and enterprises, transportation facilities, educational institutions, tourist attractions, living services, and residential areas.

3.3.3 | Road Density

The road network data utilized in this study was obtained from Open Street Map, which is a collaborative, open-source platform for mapping data. The data includes valuable information such as road names, types, and geometric coordinates. The road density for the geographical grid was calculated by dividing the total length of all types of roads, including motorways, highways, main or national roads, secondary or regional roads, and other urban and rural roads, by its surface area.

3.3.4 | River Density

River network data was also downloaded from Open Street Map. Similarly, the river density of the grid is calculated as the ratio of the total length of all rivers to its area.

3.3.5 | Meteorological Data

Hourly precipitation, average visibility, average wind speed, instantaneous temperature, and ground pressure data were sourced from the China Meteorological Administration, which is available online at http://data.cma.cn/en (see in Appendix Table A2). Additionally, this study assumes that rainfall is uniformly distributed across the study area. This assumption is based on verified observations which indicate that the 40-h accumulated rainfall between 0800 BST on 19 July and 0000 BST on 21 July 2021 was uniformly distributed and exceeded 400 mm in the central districts of Zhengzhou [48].

4 | Methodology

4.1 | Analytical Framework

This study proposes an analytical framework to characterize the response of urban travel to rainfall events. The framework comprises three modules, as illustrated in Figure 3. In the first module, the study area is divided into grids of size 1000 m × 1000 m, and trip characteristics are calculated for each grid during the study period. Specifically, time series data on the number of daily trips (sum of departures and arrivals) are collected before, during, and after the rainfall event. The k-shape clustering algorithm is then employed to classify the grids into different clusters based on their response to the rainfall impact. In the second module, multinomial logit modelling is used to evaluate the impact of built environment factors on the variability of response patterns. Finally, binary logit modelling is utilized to analyse the response of different trip types to red rainfall warnings, including changes in the number of trips. The details of the proposed framework are elaborated in the subsequent sections.

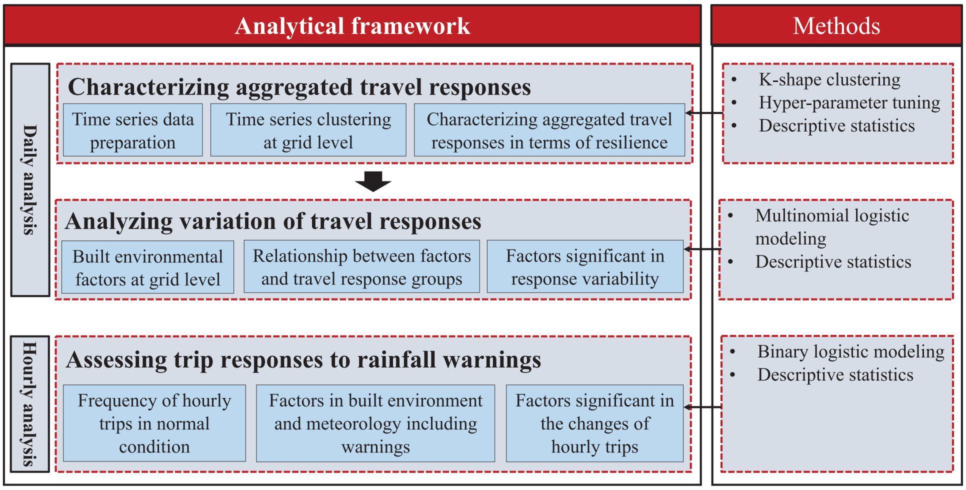

FIGURE 3 | Analytical framework.

4.2 | Characterizing Aggregated Travel Responses

The K-shape clustering algorithm is a sophisticated technique that is well-suited for clustering time series data. Compared with K-means clustering algorithm, the advantage of K-shape clustering algorithm is to calculate distance by shape (cross-correlation distance). It considers the scale invariance and translation invariance of time series, so it can better handle time series data with different amplitudes and phase differences. In this study, the K-shape algorithm is used to cluster the travel response patterns of grids.

In this study, the K-shape algorithm is used to cluster the travel response patterns of grids. This approach is appropriate because the algorithm is capable of clustering sequences with similar patterns based on their shape similarity, while being robust to differences in magnitude and phase. Additionally, urban travel responses, measured in terms of trip numbers, exhibit spatial-temporal perturbations due to heavy rainfall and pluvial flooding. Moreover, the effectiveness of the K-Shape algorithm has been demonstrated through experimental evaluation on 48 datasets [18]. This evaluation also indicates that the state-of-the-art cross-correlation-based similarity measure is competitive, outperforms the Euclidean distance, and achieves similar results to constrained dynamic time warping, without requiring complicated tuning, and performing one order of magnitude faster [18].

The key steps in K-shape clustering consist of shape-based distance (SBD) measure and time series shape extraction. SBD is based on cross-correlation, a statistical measure by which the similarity of two sequences can be determined. In detail, given two time series $\vec{x} = (x_1, x_2, \dots, x_m)$ and $\vec{y} = (y_1, y_2, \dots, y_m)$, the cross-correlation similarity between them can be calculated by Equation (1). Where the length of the similarity sequence $\mathrm{CC}_w(\vec{x}, \vec{y})$ is $2m-1$, $w \in \{1, 2, \dots, 2m-1\}$. The elements of $CC_w(\vec{x}, \vec{y})$ are derived by holding $\vec{x}$ static, sliding $\vec{y}$ over $\vec{x}$ and calculating the inner product of each shift. To meaningfully compare the input sequences, cross-correlation similarity is further normalized as shown in Equation (3), and the SBD is derived as in Equation (4), taking values from 0 to 2, a smaller value of SBD indicating a higher degree of similarity between the two sequences.

$$\mathrm{CC}_w\left(\vec{x}, \vec{y}\right) = R_{w-m}\left(\vec{x}, \vec{y}\right) \tag{1}$$

$$R_k\left(\vec{x}, \vec{y}\right) = \begin{cases} \sum_{l=1}^{m-k} x_l + k \cdot y_l \; k \geq 0 \\ R_{-k}\left(\vec{y}, \vec{x}\right) \; k < 0 \end{cases} \tag{2}$$

$$\mathrm{NCC}_w\left(\vec{x}, \vec{y}\right) = \frac{\mathrm{CC}_w\left(\vec{x}, \vec{y}\right)}{\sqrt{R_0\left(\vec{x}, \vec{x}\right) \cdot R_0\left(\vec{y}, \vec{y}\right)}} \tag{3}$$

$$\mathrm{SBD}\left(\vec{x}, \vec{y}\right) = 1 - \max\left(\mathrm{NCC}_w\left(\vec{x}, \vec{y}\right)\right) \tag{4}$$

Time series shape extraction is the second step in k-shape clustering, by selecting the centroids that reflect the class shape and characteristics. The simplest way to extract the centroids of a set of sequences is to calculate the arithmetic mean of the corresponding coordinates of all the sequences, which is popular in clustering methods such as k-means. However, such centroids cannot capture class characteristics effectively [18]. To avoid such problems, as shown in Equation (5), the extraction of the centroids is defined as an optimization problem by k-shape, with the objective of finding the data point that maximizes the sum of squared similarities to all other time sequences. where C_j represents the jth cluster and μ_j is the initial centroid of the jth cluster. The centroids are updated continuously during the optimization iterations, and the centroids from the previous iteration are used as a reference to cluster similar time sequences in the next iteration.

$$\mu_j^* = \arg\max_{\mu_j} \sum_{x \in C_j} \left(\mathrm{NCC}_w\left(\boldsymbol{x}, \mu_j\right)\right)^2 \tag{5}$$

The K-Shape clustering algorithm utilizes the SBD distance measure and shape extraction to achieve clustering through an iterative refinement process. In each iteration, the algorithm performs two steps: (i) the assignment step, where the algorithm updates the cluster memberships by comparing each time series with all computed centroids and assigns each time series to the cluster of the closest centroid; (ii) the refinement step, where the cluster centroids are updated to reflect the changes in cluster memberships from the previous step. The algorithm continues these two steps until there is no change in cluster membership or the maximum number of iterations is reached. The output of the algorithm is the assignment of sequences to clusters and the centroids for each cluster.

This study employs daily trip numbers of grids as input sequences. Due to the low dimensionality of the input data, k-shape clustering is directly applied to the raw sequence data, and the elbow method based on the sum of distances of samples to their closest cluster centre (inertia) is used to determine the optimal number of clusters. Specifically, the k-shape clustering method is run for k values ranging from 1 to 10, and the inertia is calculated for each k value. To address inconsistencies resulting from random initialization of the input sequences into defined clusters, the k-shape algorithm is executed 100 times with different centroid seeds for each k value selected in this study. This is done by randomly selecting k observations (rows) from the data as initial centroids at each execution and setting the maximum number of iterations to 1000. The final result is the best output from the consecutive runs in terms of inertia.

To address the aspect of determining the optimal number of clusters, we integrated the elbow method into our analysis, which is a technique commonly employed in various clustering algorithms, including k-shape. The elbow method involves plotting the within-cluster sum of squares (WCSS) or inertia values against the number of clusters. This graphical representation allows us to discern a point in the plot where the rate of decrease in WCSS begins to decelerate, forming an apparent "elbow" in the graph. This pivotal point signifies the optimal number of clusters for the given dataset. By employing the elbow method, we effectively strike a balance between the peril of having too few clusters, which might oversimplify the data, and the risk of having too many clusters, which might lead to excessive fragmentation.

4.3 | Analysing Variation of Travel Responses

The analytical framework developed in this study utilizes multinomial logistic regression, a widely used statistical approach in transportation studies, to examine the relationship between built environment characteristics and travel perturbations. In the model, the environmental characteristics of the grid are described by numerical variables, including the number of various types of POI (as introduced in Section 3.3), road network density, and river density, which are treated as independent variables, while clustering classes regarding travel responses are treated as dependent variables. This results in a total of nine independent variables in the model. The log-odds of a given clustering class are represented by the linear combination of these independent variables, from which key factors affecting travel perturbation and recovery can be quantified. The subsequent sections present detailed modelling results and discussion.

4.4 | Assessing Trip Responses to Rainfall Warnings

Logistic regression is utilized to evaluate the response of various trip types to red rainfall warnings. This is achieved by conducting a case study of changes in the number of trips in Zhengzhou on 20 July, during which 6 red warnings were issued based on rainfall trends. The study area's normal weekday trip frequency is recorded, and hourly frequency intervals are formed, including the maximum and minimum number of trips. If the number of trips in a given hour on 20 July falls below the lower limit of the corresponding interval, the hour is labelled as "decreased," and conversely, as "not decreased." Logistic regression modelling is conducted with the class labelled "not decreased" as the reference class, enabling analysis of the red rainfall warning's significant impact on changes in different trip types.

The modelling process considers both built environment and meteorological factors, including hourly rainfall, wind speed, and warning times, as independent variables, while hourly labels serve as dependent variables. The modelling is conducted at the grid level, with the number of warnings issued in each hour corresponding to the warning times. The analysis results are crucial in informing emergency decisions for comparable disaster scenarios in the future. For instance, based on the results, emergency personnel and supplies should be prioritized for areas that are less sensitive to warnings.

5 | Results

5.1 | Aggregated Responses of Urban Travel

Drawing upon the clustering process discussed in Section 4.2, we analysed the aggregated travel responses in the study area. The relationship between the number of clusters and the inertia values is presented in Figure A1 in the Appendix. As the number of clusters (k) increases, the subdivision of the sample dataset becomes progressively finer, leading to a heightened level of granularity in each cluster's composition. This refinement naturally results in a reduction in the sum of distances between individual samples and their respective cluster centres, a metric commonly referred to as inertia. Notably, an observable trend emerges: when k is less than 4, the increase in k corresponds to a more substantial reduction in inertia, primarily attributable to the enhanced cohesion of cluster constituents. Conversely, when k exceeds 4, the diminishing rate of Inertia reduction becomes increasingly pronounced with rising k. In light of this analysis, we opted to conduct our clustering with k set at 4, a decision substantiated by the subsequent findings presented in Figure 4. Employing the k-shape based clustering algorithm with k equal to 4, we unveil a clear delineation of four distinct groups, each epitomizing comparable patterns of travel response and recovery at the granularity of geographic grid units. This clustering arrangement effectively captures the temporal dynamics of three essential phases in disaster response: pre-event equilibrium, event-induced impact, and the subsequent recovery, as vividly illustrated in the results. Qualitative analysis reveals that trips on weekends (July 17–18) in cluster 1 are greater than weekdays (July 12–15) in the normal period, and the number of trips is relatively small. However, trips in clusters 2–4 are higher on weekdays than weekends. During the period of concentrated rainfall (July 19–20), the decrease in trips is noticeable across all clusters. It is worth noting that the upward trend observed in Cluster 3 during the disaster was influenced by the government's mandatory evacuation order, given the overlap of the spatial distribution

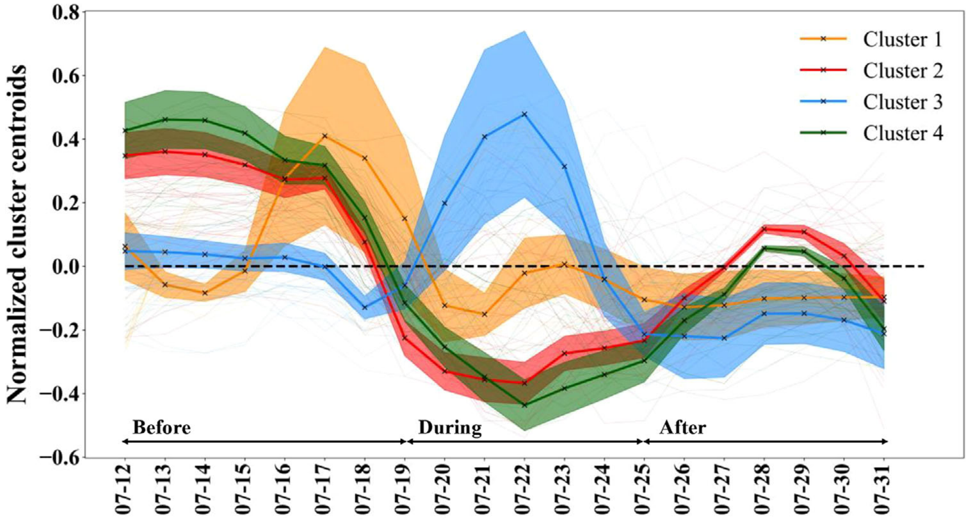

FIGURE 4 | Clustering results.

of Cluster 3 with the evacuation locations (available at: http://www.gov.cn/fuwu/2021-07/21/content_5626346.htm). Moreover, the recovered trips from the 22nd are perturbed by the light rainfall from July 23 to 24, and the gradual recovery process begins on the 25th.

Building upon the results of the clustering analysis, we further categorized the types of travel responses in terms of resilience. Resilience can generally be defined as the ability of a system to withstand the effects of a disruptive shock and recover to its initial state [49, 50]. Therefore, urban travel resilience can be described as the ability of individuals to withstand the impact of public crises and maintain normal mobility behaviour [40, 51]. Following this definition, a grid is considered to have high travel resilience if it experiences less of a decline in the number of trips and recovers quickly under the influence of extreme precipitation. Specifically, using weekdays as the reference, we found that Cluster 1 experienced a 38.6% decrease in average trips during the disaster (July 19–23) and a 62.1% recovery after the disaster (July 26–30), compared to the pre-disaster period (July 12–16). Similarly, Cluster 2 had a 23.3% decrease in average trips during the disaster and an 89.4% recovery after the disaster, while Cluster 3 showed a statistical result of a −17.4% decline and an 86.5% recovery. As previously mentioned, the 17.4% increase in Cluster 3 resulted from government evacuation orders. Cluster 4 had a similar centroid curve to Cluster 2 but experienced a greater decline and slower recovery in average trips, with a 32.6% decrease and a 77.8% recovery, respectively. Finally, we defined the grids in each cluster as follows:

- Low travel resilience (cluster 1, including 72 grids);
- High travel resilience (cluster 2, including 564 grids);
- Medium travel resilience (cluster 3, including 195 grids);
- Moderate travel resilience (cluster 4, including 308 grids).

In addition to temporal heterogeneity, travel response also exhibits spatial heterogeneity, as shown in Figure 5, which displays the spatial distribution of clusters. It is evident that the grids in cluster 1 are primarily located in suburban tourist attractions, such as parks near rivers, while cluster 3 is also mostly situated in suburban areas. The grids in cluster 2 and cluster 4 are distributed from the city centre to the suburbs, and their spatial distribution is similar. Appendix Table A1 highlights that the average number of POIs in both cluster 2 and cluster 4 is higher than that in cluster 1 and cluster 3. Additionally, the average amounts in cluster 4 are higher than those in cluster 2. Furthermore, the grids in cluster 4 have an average road network density of 7.98, which is higher than that of the other clusters. It is somewhat counterintuitive that grids with high numbers of transit facilities and roadway density, on average, lead to moderate travel resilience. To avoid analytical bias caused by arithmetic averaging, the next section presents an analysis of the factors influencing travel resilience at the grid level.

5.2 | Potential Impact Factors in the Variation of Travel Responses

After considering variables related to the built environment characteristics, we conducted an analysis of potential factors that may impact travel responses or travel resilience, and the results are presented in Table 1. As the grids in cluster 1 primarily consist of suburban recreational sites, such as green areas and parks, and are limited in number, they were not included in this study. Overall, our analysis suggests that road network density is a crucial factor in promoting travel resilience against extreme precipitation events, while river density has a negative impact on travel resilience. Additionally, areas with higher numbers of administrative institutions, amenities, and residential facilities appear to have relatively high travel resilience. In contrast, the number of transportation ancillary facilities, such as bus/metro stops, parking lots, and community entrances/exits, did not have a significant effect on travel resilience.

Our analysis reveals that several variables are significant, including road density, water density, numbers of administrative agencies, educational institutions, tourist attractions, living services, and residential facilities in the grids, when taking cluster

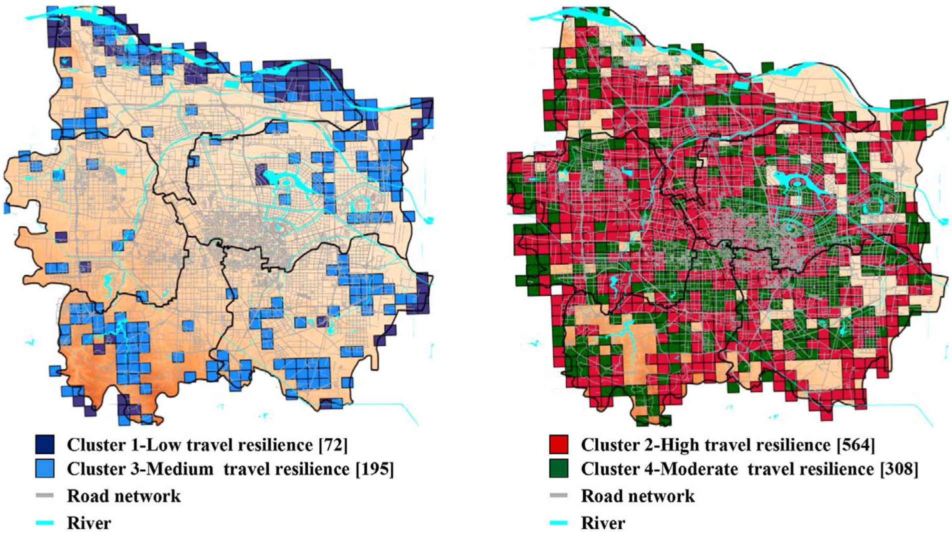

FIGURE 5 | Spatial distribution of identified clusters.

TABLE 1 | Logistic regression analysis results for travel responses.

	Cluster 3		Cluster 4	
	Coef	$P > \|z\|$	Coef	$P > \|z\|$
Administrative agencies	**−0.028**	**0.091***	**−0.006**	**0.331**
Companies and enterprises	0.002	0.273	−0.004	0.001**
Transportation facilities	**0.001**	**0.958**	**0.009**	**0.000****
Educational institutions	**0.033**	**0.002****	**0.008**	**0.033****
Tourist attractions	−0.205	0.007**	0.076	0.020**
Living services	**−0.005**	**0.000****	**−0.001**	**0.824**
Residential facilities	**−0.142**	**0.000****	**−0.008**	**0.321**
Road density	**−0.043**	**0.003****	**−0.024**	**0.047****
River density	**0.016**	**0.004****	**0.002**	**0.825**
Const	0.746	0.585	0.013	0.007

Note: Number of observations = 1139; reference class = cluster 2; pseudo R-squared = 0.1042. $P < 0.05$**; $p < 0.1$*.

2 as the reference class. Specifically, for cluster 3, a negative coefficient indicates that an increase in the variable will decrease the probability of it being selected relative to cluster 2, while a positive coefficient indicates the opposite. For instance, a one-unit increase in road network density in the grid of cluster 3 would reduce the multinomial log-odds for cluster 3 relative to cluster 2 by 0.043 units while keeping all other variables constant, indicating the critical role of road network density in promoting travel resilience. These findings align with previous studies by He et al. [52] and Kasmalkar et al. [53], which demonstrate that higher road density can improve overall network resilience and significantly reduce the risk of mobility disruptions, such as trip failures. Furthermore, our analysis indicates that river density has a negative impact on travel resilience, as indicated by the positive coefficient of 0.016. This may be due to the fact that rivers serve as outlets for urban drainage, and extreme rainfall events can cause river overflow, leading to a capacity degradation of nearby transportation facilities.

Likewise, our analysis shows that in cluster 3, the negative coefficients for the number of administrative agencies, living services, and residential facilities suggest that areas with a higher concentration of these facilities tend to have greater resilience to extreme rainfall events relative to cluster 2 (i.e. high resilience). This trend can also be observed in cluster 4, although the coefficient is not statistically significant. Notably, the positive coefficients for the number of educational institutions in clusters 3 and 4 suggest that grids with a larger number of educational facilities have relatively lower travel resilience. This may be due to delayed school openings for safety reasons or restricted access to universities due to rainfall and flooding. Additionally, our modelling results indicate that the number of bus/metro stops and parking lots in the grid do not significantly contribute to travel resilience, which is unsurprising given that travel is dependent on the mode of transportation rather than ancillary facilities. The role of road network density in enhancing travel resilience is further supported by our findings in cluster 4

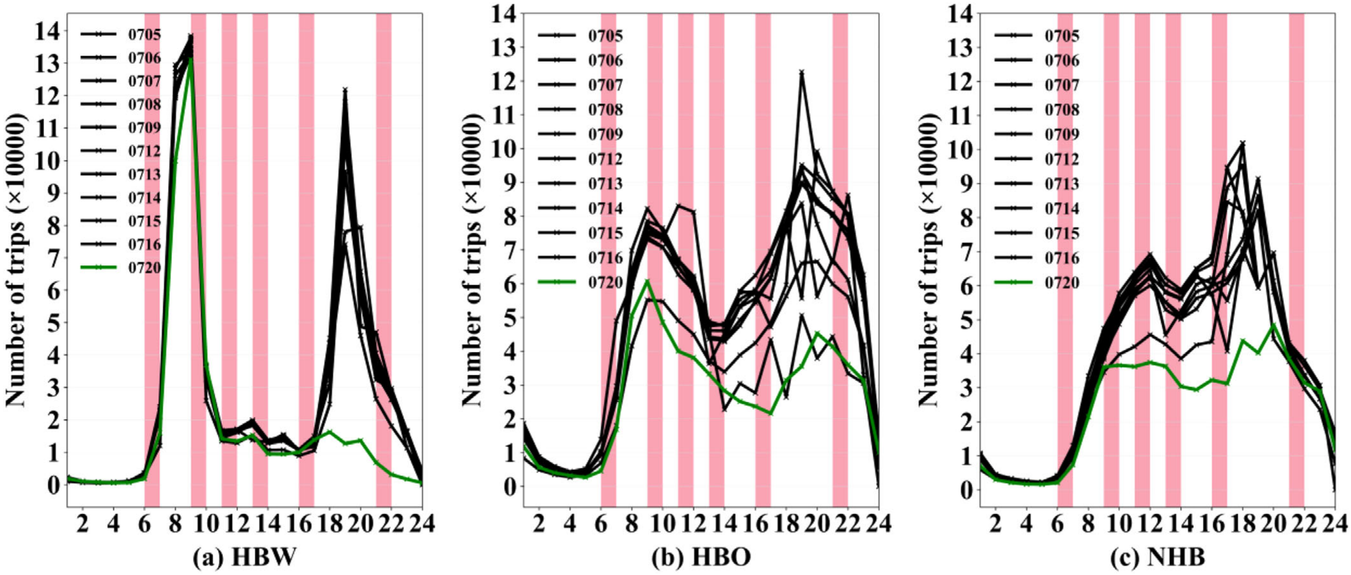

FIGURE 6 | Change in number of hourly trips (each vertical pink shaded area represents a red rainstorm warning, and a total of 6 red rainstorm warning signals were issued on July 20).

when compared to the reference class. Moreover, although the coefficient is not statistically significant, the positive coefficient for river density in cluster 4 validates its negative impact on urban travel.

5.3 | Responses of Trip Types to Rainfall Warnings

To examine the impact of red rainfall warnings on different trip types, we first determined whether the hourly trips on the 20th were below the normal hourly frequency intervals. The frequency intervals were established by using ten weekdays from the 2 weeks prior to the 20th as the reference normal period. Figure 6 displays the changes in the number of trips for different trip types on the 20th day compared to the reference days. Our analysis reveals that home-based work trips (HBW) or non-mandatory trips appear to be less affected by red rainfall warnings. Specifically, for HBW trips, a significant decrease in the number of trips is observed during the fifth warning period (16:00–17:00), which coincides with the maximum hourly rainfall. In contrast, for home-based other trips (HBO) and non-home-based trips (NHB), a significant reduction in the number of trips is observed after the issuance of the first warning. This could suggest that both the issuance of the warning and the volume of rainfall can influence these types of trips, unlike HBW trips where the volume of rainfall may have a greater impact than the warning.

To investigate the responses of different travel types, we examined the mediating effects of built environment characteristics, hazard characteristics, and government warnings. In this section, we focused on built environment characteristics, such as the amount of POI types and road network density, as well as hazard characteristics, including the amount of rainfall per hour on the 20th. These factors were analysed using the same methodology as described in Section 4.4, and the modelling results are summarized in Table 2. Our findings indicate that for all trip types, areas with a high number of POI types, including administrative agencies, companies and enterprises, transportation facilities, educational institutions, and residential facilities, are more likely to experience a decrease in the number of trips. This is evidenced by the positive modelling coefficients relative to the reference class of "not decreased". Additionally, road density also shows a mediating effect on the reduction in the number of trips. This aligns with the empirical observation that areas with high POI amounts tend to have relatively high road network densities, which contribute to impervious surfaces and hinder water infiltration, ultimately leading to increased road surface runoff during extreme rainfall conditions [54–56].

Furthermore, our modelling results indicate that HBW trips are less affected by rainfall warnings compared to HBO and NHB trips. Specifically, the impact of the number of warnings per hour on the decline of HBW trips is not significant at the 95% confidence level, which differs from the case of HBO and NHB trips. These findings are consistent with previous studies, such as Cools and Creemers, [57], which analysed the role of weather forecasts or warnings on changes in activity-travel behaviour based on questionnaires. The study revealed that travellers do adjust their activity-travel patterns, particularly for trips with non-mandatory purposes (e.g. shopping and leisure), which are more flexible than commuting in responding to changes in weather conditions [58].

6 | Discussions

In recent years, there has been a noticeable increase in the frequency and intensity of EWEs across the globe [40]. This trend is expected to continue and intensify in the future [40, 59], posing significant challenges for urban travel. EWEs such as heavy rainfall can lead to a reduction in transportation supply capacity and a change in activity-travel behaviour, making emergency management more complex for policymakers due

TABLE 2 | Logistic regression analysis results for warning responses.

	Home-based work		Home-based other		Non-Home-based other	
	Coef	***P* > |*z*|**	**Coef**	***P* > |*z*|**	**Coef**	***P* > |*z*|**
Administrative agencies	0.003	0.131	0.005	0.003**	0.004	0.015**
Companies and enterprises	0.002	0.000**	0.001	0.000**	0.001	0.001**
Transportation facilities	0.002	0.016**	0.004	0.000**	0.003	0.000**
Educational institutions	0.005	0.000**	0.002	0.073*	0.004	0.000**
Tourist attractions	−0.006	0.454	0.007	0.114	−0.002	0.698
Living services	−0.005	0.078	−0.001	0.541	0.001	0.000**
Residential facilities	0.001	0.784	0.003	0.147	0.001	0.689
Road density	0.065	0.000**	0.048	0.000**	0.052	0.000**
River density	−0.019	0.000**	−0.021	0.000**	−0.019	0.000**
Hourly warning	0.069	0.097*	0.281	0.000**	0.283	0.000**
Hourly wind	−0.092	0.000**	0.109	0.000**	0.159	0.000**
Hourly precipitations	0.019	0.000**	0.004	0.000**	0.005	0.000**
Const	−1.684	0.000**	−2.426	0.000**	−2.762	0.000**

Note: Number of observations = 27,336, derived by 1139 grids x 24 h; Reference class = " not decreased "; Pseudo R-squared = 0.119, 0.124, 0.195. $P < 0.05$**; $p < 0.1$*.

to their high uncertainty and destructiveness. The importance of understanding urban travel responses under the impact of EWEs cannot be overstated, as it plays a critical role in disaster mitigation and preparedness [2, 4]. Recent research leveraging diverse forms of human trajectory data, encompassing cellphone records, GPS vehicle and pedestrian trajectories, and online social media check-ins, has made substantial strides in advancing our comprehension of prevailing human mobility patterns within urban contexts. This research endeavour has yielded a repository of objective, generalizable, and scalable metrics for gauging resilience to various hazards and their ramifications, thoughtfully considering the intricate spatiotemporal dynamics intrinsic to localized responses to and recovery from these hazards. Exemplifying this progress, studies conducted by Hong et al. (2020) and Zhang et al. [40] undertook an insightful examination of mobility patterns amidst disaster events, such as Hurricane Harvey in Houston and extreme weather occurrences in Nanjing, respectively. Notably, these investigations construed the concept of community resilience by scrutinizing alterations in mobility behaviour preceding, coinciding with, and subsequent to disasters, facilitating a quantitative assessment of both the magnitude of impact and the temporal aspects of recovery. Furthermore, the study undertaken by Chen et al. [1] delved into the repercussions of extreme weather events on disruptions in urban pedestrian flow, with particular emphasis on the context of Typhoon Mangkhut's impact in Shenzhen, China. The findings stemming from this research unveiled the relative robustness of indispensable urban functions, such as work-related and education-related travel, in the face of such disruptions. In summation, these studies culminate in the extraction of invaluable insights from location-based data, unravelling the facets characterizing the collapse of mobility, thus proffering essential guidance to urban planners and policymakers in their pursuit of fortifying urban disaster resilience. It is important to underscore that this research is notably complementary to the existing literature, as it addresses the unique context of heavy rainfall scenarios.

This study examines the impact of extreme rainfall on urban travel through the analysis of cell phone signalling-based mobility big data. The findings are consistent with above studies. The analysis identifies four distinct groups of travel responses based on clustering algorithm *k*-shape, representing similar patterns of disaster response and recovery at the grid level. The descriptive analysis of the built environment characteristics of the clusters reveals spatial heterogeneity, which leads to temporal heterogeneity of responses. Furthermore, the study shows that built environment factors affect travel resilience. For example, areas with higher numbers of administrative institutions, living facilities, and residential facilities appear to have higher travel resilience. Similarly, studies by Podesta et al. [60] show that areas with large numbers of POIs, such as administrative agencies, building materials and supplies dealers, and grocery and merchandise stores, have higher flood resilience. One possible reason is that food, supplies, and restoration activities related trips to meet core basic and safety needs contribute to recovery. Of particular concern, the study also reveals that road network density has a dual impact on community travel resilience. On the one hand, road network density positively affects travel resilience in the long term from pre-disaster to recovery. On the other hand, hourly-based analysis shows that areas with high road network density have a faster decline in all types of trips during the initial stages of the disaster. Previous studies also suggest similar findings, such as higher road network density reducing the likelihood of flooding and acting as a disincentive for flooding [61]. However, some studies suggest that flooding increases with road network density, as roads may affect the amount of infiltrated water [62]. The divergence of the findings may be dependent on the time scale of the analysis. Specifically, the hourly analysis in Section 5.3 is based on the day of the disaster

(July 20th), which recorded the highest hourly rainfall. While the analysis in Section 5.2 is based on the time period affected by the rainfall spanning from the 19th to the 25th. That is, areas with higher road network density are more vulnerable at the onset of the disaster. However, taking a long-term perspective, higher road network density contributes to faster recovery and more robust travel resilience.

The analysis of weather forecasts or warnings on trip changes provides important insights into travel responses during extreme weather events. The study reveals that home-based work (HBW) trips are less sensitive to rainfall warnings compared to home-based other (HBO) and non-home-based (NHB) trips. Such findings have significant implications for disaster mitigation and preparedness. For example, emergency resources such as pumpers and emergency staffing should be prioritized in areas and corridors where HBW trips are more intensive. Additionally, as an important tool for government and public agencies to interfere with the avoidance behaviour of individuals [2, 57], six red rainfall warnings were issued on the day of the disaster (20th) in Zhengzhou. However, the results of the case study and the disaster losses already reported in the news, including drownings on Metro Line 5 and the Jing-guang Expressway after the 5th warning, may reveal the inadequate effectiveness of the warning dissemination. Specifically, the six red warnings were issued with the expression "Rainfall amounts could exceed 100 mm in the coming 3 h ", and there was no difference in the expression of the 5th warning issued at 16:00 on the 20th when the extreme 1-h rainstorm peak of over 200 mm was about to land. This may make it difficult for the public to feel the urgency and seriousness of the approaching risk, but may be negligent because no serious consequences were found after the first 4 warnings. Since personal risk perception and self-efficacy are key factors in flood warning response [63, 64].

Previous studies have shown that the effectiveness of warnings during disasters depends not only on the disaster types and severity but also on the content, format, and dissemination channels of the warnings [57, 65, 66]. For example, the combination of affective language style and images can increase the effectiveness of warnings [65, 67, 68]. Moreover, the incorporation of impact-based warnings and behavioural recommendations into warning messages has shown advantages [69–72]. The study highlights the need for a more detailed and comprehensive approach to warning dissemination to ensure that the public is adequately informed of the risks and takes appropriate measures to mitigate the impact of extreme weather events. In the case of the Zhengzhou floods, more detailed analysis based on the information of the precursors of the approaching heavy rainfall could have resulted in more effective warnings. For instance, the warnings issued could have included the accumulated rainfall in the early period or potentially affected roads. The findings of this study provide practical policies and recommendations for government agencies and road users.

For government agencies:

1. Prioritize emergency resources in areas with intensive home-based work (HBW) trips during extreme weather events to ensure rapid disaster response.
2. Improve the effectiveness of warning dissemination by considering not only the severity of the disaster but also the content, format, and channels used for warnings. Utilize affective language style, images, and impact-based warnings to enhance public awareness and response.
3. Conduct more detailed and comprehensive analyses of impending extreme weather events, including precursor information like accumulated rainfall and potentially affected roads, to issue more effective warnings.

For road users:

1. Pay special attention to red rainfall warnings, especially when they indicate severe rainfall amounts or abrupt changes in weather conditions.
2. Take personal risk perception and self-efficacy into account when responding to flood warnings. Understand that the lack of serious consequences after initial warnings does not necessarily indicate reduced risk.
3. Stay informed about disaster-related warnings through multiple channels and sources to ensure timely and accurate information. Follow recommended behavioural guidelines in response to warnings to enhance personal safety during extreme weather events.

7 | Conclusions

This paper presents a comprehensive case study aimed at assisting urban policy makers in understanding the aggregated responses of urban travel under the impact of extreme rainfall and its associated hazards. To achieve this, cell phone signalling-based mobility big data was collected during the perturbations and used as the basis for analysis. Furthermore, a shape-based time series clustering algorithm and sophisticated discrete choice modelling techniques were employed to analyse the data, with the 2021 Zhengzhou floods serving as a case study. Specifically, the study utilized grid aggregated trips as input and identified four distinct groups that demonstrate similar response and recovery patterns using the k-shape clustering algorithm. The heterogeneity observed within these groups could be attributed to built environment factors such as road network density. Furthermore, the study analysed the response of different trip types to red rainfall warnings, with the day of the disaster serving as a case study. Overall, this study provides valuable insights into the aggregated responses of urban travel during extreme rainfall events and can assist policy makers in developing effective strategies to mitigate the impact of such hazards.

The research methodology employed in this study offers valuable insights into urban travel responses during extreme rainfall events, shedding light on vulnerability and resilience in urban areas. However, it is essential to acknowledge several limitations: (1) data constraints and explanatory factors: the study primarily focuses on built environment factors due to data constraints. This limitation may lead to an incomplete understanding of the spatial-temporal heterogeneity of travel responses. Future research should consider incorporating additional variables such as historical waterlogging frequency, economic level, and community-related factors to provide a more comprehensive and robust analysis. (2) Evacuation orders and cluster 3: The study mentions obtaining evacuation orders from government websites and social media during the disaster. However, it is challenging to differentiate whether the increased trips in cluster 3 were due to community recovery or the activities of emergency response teams, which also involve a significant number of trips. This ambiguity can impact the accuracy of the findings and the interpretation of results. (3) Post-flood recovery process: While the study observes an increase in trips during the post-flood recovery process, it lacks a comprehensive explanation of how the area returned to normalcy. The absence of follow-up data limits the ability to analyse the process and characteristics of recovery fully. Future research should address this by incorporating follow-up data and providing a more detailed account of the recovery phase. In summary, while the research methodology has yielded significant findings, these limitations should be considered when interpreting the results and planning future studies. Addressing these limitations will enhance the robustness and applicability of the research for urban policy makers and emergency response planning.

It is important to acknowledge that our study has there are several promising avenues for future work to expand and improve our understanding of urban travel responses and disaster mitigation. (1) Multi-dimensional factors: future research can broaden the scope of explanatory factors influencing travel responses. In addition to built environment factors, as mentioned in the study, researchers can explore the influence of historical weather events, economic indicators, and community-related factors on urban travel responses. This will result in a more comprehensive analysis, considering a wider range of variables that impact resilience and vulnerability. (2) Real-time data and activity differentiation: To enhance the accuracy of cluster analysis and response attribution, incorporating real-time data sources and advanced machine learning techniques could be considered. This can help differentiate between community recovery and the activities of emergency response teams, ensuring that the increase in trips within specific clusters is correctly attributed. (3) Post-disaster recovery process: To gain a more holistic understanding of the post-disaster recovery process, future studies should focus on collecting follow-up data and conducting a detailed analysis of how areas return to normalcy. This can involve monitoring travel patterns, infrastructure restoration, and community rehabilitation, providing valuable insights for long-term resilience planning. (4) Comparative Studies: Comparative studies involving multiple cities or regions that have experienced extreme weather events can provide a broader perspective on the impact of built environment factors and emergency response strategies. Analysing similarities and differences across various urban contexts can lead to more generalizable findings and help identify best practices. (5) Communication strategies: Building on the study's findings on the sensitivity of different trip types to rainfall warnings, future research can delve deeper into the effectiveness of communication strategies during extreme events. This may involve experimenting with different warning formats, channels, and content to optimize public response and decision-making. In summary, there are several exciting avenues for future work in the field of urban travel responses to extreme weather events. By expanding the scope of variables, leveraging real-time data, and conducting comparative studies, researchers can contribute to more effective disaster mitigation strategies and long-term urban resilience planning.

Author Contributions

Qian Ye: conceptualization, formal analysis, writing – original draft. **Yulin Ma:** data curation, supervision. **Shucai Xu:** investigation, writing – review & editing. **Miguel Sotelo:** writing – review & editing. **Zhixiong Li:** formal analysis.

Conflicts of Interest

The authors declare no conflicts of interest.

Data Availability Statement

The data used to support the findings of this study are available from the corresponding author upon request.

Endnotes

[1] The red rainfall warning is the warning signal issued by the meteorological department before the arrival of the rainstorm, reminding people to avoid rainstorm. Red rainfall warning means the precipitation will reach over 100 millimeters within 3 h, which is the fourth and most serious level of rainstorm warning signal.

References

1. Z. Chen, Z. Gong, S. Yang, Q. Ma, and C. Kan, "Impact of Extreme Weather Events on Urban Human Flow: A Perspective From Location-Based Service Data," *Computers, Environment and Urban Systems* 83 (2020): 101520, https://doi.org/10.1016/j.compenvurbsys.2020.101520.

2. C. Xia and A. G. O. Yeh, "Mobility as a Response to Environmental Hazards in the Urban Context: A New Perspective on Mobility and Inequality," *Travel Behaviour and Society* 27 (2022): 192–203, https://doi.org/10.1016/j.tbs.2022.01.008.

3. M. A. Ahmed, K. Haynes, and M. Taylor, "Driving Into Floodwater: A Systematic Review of Risks, Behaviour and Mitigation," *International Journal of Disaster Risk Reduction* 31 (2018): 953–963, https://doi.org/10.1016/j.ijdrr.2018.07.007.

4. B. Hong, B. J. Bonczak, A. Gupta, and C. E. Kontokosta, "Measuring Inequality in Community Resilience to Natural Disasters Using Large-Scale Mobility Data," *Nature Communications* 12 (2021): 1870, https://doi.org/10.1038/s41467-021-22160-w.

5. H. A. Simon, "A Behavioral Model of Rational Choice," *Competition Policy International* 6, no. 1 (1957): 317–344.

6. D. Kahneman and A. Tversky, 2013. Choices, Values, and Frames. in Handbook of the Fundamentals of Financial Decision Making (World Scientific, 2013), 269–278.

7. K. T. Huang, "Mapping the Hazard: Visual Analysis of Flood Impact on Urban Mobility," *IEEE Computer Graphics and Applications* 41 (2021): 26–34, https://doi.org/10.1109/MCG.2020.3041371.

8. X. Zhang and N. Li, "Characterizing Individual Mobility Perturbations in Cities During Extreme Weather Events," *International Journal of Disaster Risk Reduction* 72 (2022): 102849, https://doi.org/10.1016/j.ijdrr.2022.102849.

9. R. P. B. Abad, T. Schwanen, and A. M. Fillone, "Commuting Behavior Adaptation to Flooding: An Analysis of Transit Users' Choices in Metro Manila," *Travel Behaviour and Society* 18 (2020): 46–57, https://doi.org/10.1016/j.tbs.2019.10.001.

10. N. Golshani, R. Shabanpour, A. Mohammadian, J. Auld, and H. Ley, "Modeling Evacuation Demand During no-Notice Emergency Events:

Tour Formation Behavior," *Transportation Research Part C: Emerging Technologies* 118 (2020): 102713, https://doi.org/10.1016/j.trc.2020.102713.

11. C. Lin, K. Wang, D. Wu, and B. Gong, "Research on Residents' Travel Behavior Under Sudden Fire Disaster Based on Prospect Theory," *Sustainability (Switzerland)* 12 (2020): 487, https://doi.org/10.3390/su12020487.

12. S. D. Wong, C. G. Chorus, S. A. Shaheen, and J. L. Walker, "A Revealed Preference Methodology to Evaluate Regret Minimization With Challenging Choice Sets: A Wildfire Evacuation Case Study," *Travel Behaviour and Society* 20 (2020): 331–347, https://doi.org/10.1016/j.tbs.2020.04.003.

13. A. Galeazzi, M. Cinelli, G. Bonaccorsi, et al., "Human Mobility in Response to COVID-19 in France, Italy and UK," *Scientific Reports* 11 (2021): 13141, https://doi.org/10.1038/s41598-021-92399-2.

14. Y. Pan, A. Darzi, A. Kabiri, et al., "Quantifying Human Mobility Behaviour Changes During the COVID-19 Outbreak in the United States," *Scientific Reports* 10 (2020): 20742, https://doi.org/10.1038/s41598-020-77751-2.

15. S. Liu, H. Jiang, and Z. Chen, "Quantifying the Impact of Weather on Ride-Hailing Ridership: Evidence From Haikou, China," *Travel Behaviour and Society* 24 (2021): 257–269, https://doi.org/10.1016/j.tbs.2021.04.002.

16. Q. Miao, E. W. Welch, and P. S. Sriraj, "Extreme Weather, Public Transport Ridership and Moderating Effect of Bus Stop Shelters," *Journal of Transport Geography* 74 (2019): 125–133, https://doi.org/10.1016/j.jtrangeo.2018.11.007.

17. M. Wei, "How Does the Weather Affect Public Transit Ridership? A Model With Weather-passenger Variations," *Journal of Transport Geography* 98 (2022): 103242, https://doi.org/10.1016/j.jtrangeo.2021.103242.

18. J. Paparrizos and L. Gravano, "K-Shape: Efficient and Accurate Clustering of Time Series," in Proceedings of the ACM SIGMOD International Conference on Management of Data (ACM, 2015), 1855–1870.

19. K. Hamilton, J. J. Keech, A. E. Peden, and M. S. Hagger, "Changing Driver Behavior During Floods: Testing a Novel E-Health Intervention Using Implementation Imagery," *Safety Science* 136 (2021): 105141, https://doi.org/10.1016/j.ssci.2020.105141.

20. T. Tang, R. Liu, and C. Choudhury, "Incorporating Weather Conditions and Travel History in Estimating the Alighting Bus Stops From Smart Card Data," *Sustainable Cities and Society* 53 (2020): 101927, https://doi.org/10.1016/j.scs.2019.101927.

21. R. Alawadi, P. Murray-Tuite, D. Marasco, S. Ukkusuri, and Y. Ge, "Determinants of Full and Partial Household Evacuation Decision Making in Hurricane Matthew," *Transportation Research Part D: Transport and Environment* 83 (2020): 102313, https://doi.org/10.1016/j.trd.2020.102313.

22. R. Bian, C. G. Wilmot, R. Gudishala, and E. J. Baker, "Modeling Household-Level Hurricane Evacuation Mode and Destination Type Joint Choice Using Data From Multiple Post-Storm Behavioral Surveys," *Transportation Research Part C: Emerging Technologies* 99 (2019): 130–143, https://doi.org/10.1016/j.trc.2019.01.009.

23. A. Pan, "Study on the Decision-Making Behavior of Evacuation for Coastal Residents Under Typhoon Storm Surge Disaster," *International Journal of Disaster Risk Reduction* 45 (2020): 101522, https://doi.org/10.1016/j.ijdrr.2020.101522.

24. S. D. Wong, J. C. Broader, J. L. Walker, and S. A. Shaheen, "Understanding California Wildfire Evacuee Behavior and Joint Choice Making," *Transportation* (2022), https://doi.org/10.1007/s11116-022-10275-y.

25. S. Thakur, P. Ranjitkar, and S. Rashidi, "Investigating Evacuation Behaviour Under an Imminent Threat of Volcanic Eruption Using a Logistic Regression-Based Approach," *Safety Science* 149 (2022): 105688, https://doi.org/10.1016/j.ssci.2022.105688.

26. S. Shapira, L. Aharonson-Daniel, and Y. Bar-Dayan, "Anticipated Behavioral Response Patterns to an Earthquake: The Role of Personal and Household Characteristics, Risk Perception, Previous Experience and Preparedness," *International Journal of Disaster Risk Reduction* 31 (2018): 1–8, https://doi.org/10.1016/j.ijdrr.2018.04.001.

27. Q. C. Lu, J. Zhang, Z. R. Peng, and A. S. Rahman, "Inter-City Travel Behaviour Adaptation to Extreme Weather Events," *Journal of Transport Geography* 41 (2014): 148–153, https://doi.org/10.1016/j.jtrangeo.2014.08.016.

28. J. Hou, W. m. Gai, W. y. Cheng, and Y. f. Deng, "Survey-Based Analysis of Evacuation Preparation Behaviors in a Chemical Leakage Accident: A Case Study," *Journal of Loss Prevention in the Process Industries* 68 (2020): 104219, https://doi.org/10.1016/j.jlp.2020.104219.

29. E. Mirzaei, R. Kheyroddin, and D. Mignot, "Exploring the Effect of the Built Environment, Weather Condition and Departure Time of Travel on Mode Choice Decision for Different Travel Purposes: Evidence From Isfahan," *Iran Case Study on Transportation Policy* 9 (2021): 1419–1430, https://doi.org/10.1016/j.cstp.2021.05.002.

30. C. Liu, Y. O. Susilo, and N. Ahmad Termida, "Weather Perception and Its Impact on Out-of-Home Leisure Activity Participation Decisions," *Transportmetrica B* 8 (2020): 219–236, https://doi.org/10.1080/21680566.2020.1733703.

31. J. Wu and H. Liao, "Weather, Travel Mode Choice, and Impacts on Subway Ridership in Beijing," *Transportation Research Part A: Policy and Practice* 135 (2020): 264–279, https://doi.org/10.1016/j.tra.2020.03.020.

32. K. Takemura, *Behavioral Decision Theory, Behavioral Decision Theory* (Springer, 2021).

33. M. van Essen, T. Thomas, E. van Berkum, and C. Chorus, "From User Equilibrium to System Optimum: A Literature Review on the Role of Travel Information, Bounded Rationality and Non-Selfish Behaviour at the Network and Individual Levels," *Transportation Review* 36 (2016): 527–548, https://doi.org/10.1080/01441647.2015.1125399.

34. D. A. Hensher, J. M. Rose, and W. H. Greene, "Applied Choice Analysis: Mixed logit estimation," (2005).

35. S. Schneider, M. Peter, M. Director, and T. Mayer. Self-Interest as a Disciplining Factor on Markets? Efficient Market Theory Misperceives the Dynamics of Economic Crises Homo Economicus Under Fire (2010).

36. G. Wang, S. Ma, and N. Jia, "A Combined Framework for Modeling the Evolution of Traveler Route Choice Under Risk," *Transportation Research Part C: Emerging Technologies* 35 (2013): 156–179, https://doi.org/10.1016/j.trc.2013.06.019.

37. S. An, Z. Wang, and J. Cui, "Integrating Regret Psychology to Travel Mode Choice for a Transit-Oriented Evacuation Strategy," *Sustainability* 7 (2015): 8116–8131, https://doi.org/10.3390/su7078116.

38. Y. Zhou, Z. Li, Y. Meng, Z. Li, and M. Zhong, "Analyzing Spatio-Temporal Impacts of Extreme Rainfall Events on Metro Ridership Characteristics," *Physica A: Statistical Mechanics and Its Applications* 577 (2021): 126053, https://doi.org/10.1016/j.physa.2021.126053.

39. R. Wang, X. Zhang, and N. Li, "Zooming Into Mobility to Understand Cities: A Review of Mobility-Driven Urban Studies," *Cities* 130 (2022): 103939, https://doi.org/10.1016/j.cities.2022.103939.

40. F. Zhang, Z. Li, N. Li, and D. Fang, "Assessment of Urban Human Mobility Perturbation Under Extreme Weather Events: A Case Study in Nanjing, China," *Sustainable Cities and Society* 50 (2019): 101671, https://doi.org/10.1016/j.scs.2019.101671.

41. A. Ahmouda, H. H. Hochmair, and S. Cvetojevic, "Using Twitter to Analyze the Effect of Hurricanes on Human Mobility Patterns," *Urban Science* 3 (2019): 87, https://doi.org/10.3390/URBANSCI3030087.

42. H. Wang, Y. Hu, Y. Guo, Z. Wu, and D. Yan, "Urban Flood Forecasting Based on the Coupling of Numerical Weather Model and Stormwater Model: A Case Study of Zhengzhou city," *Journal of Hydrology: Regional Studies* 39 (2022): 100985, https://doi.org/10.1016/j.ejrh.2021.100985.

43. Q. Zheng, S. L. Shen, A. Zhou, and H. M. Lyu, "Inundation Risk Assessment Based on G-DEMATEL-AHP and Its Application to Zhengzhou Flooding Disaster," *Sustainable Cities and Society* 86 (2022): 104138, https://doi.org/10.1016/j.scs.2022.104138.

44. F. Wang, J. Wang, J. Cao, C. Chen, and X. (J.) Ban, "Extracting Trips From Multi-Sourced Data for Mobility Pattern Analysis: An App-Based Data Example," *Transportation Research Part C: Emerging Technologies* 105 (2019): 183–202, https://doi.org/10.1016/j.trc.2019.05.028.

45. Transportation Research Board, *Does the Built Environment Influence Physical Activity?: Examining the Evidence—Special Report 282* (Institute of Medicine of the National Academies, 2005).

46. M. Yin, S. M. Qiao, S. Feygin, J.-F. Paiement, and A. Pozdnoukhov, "A Generative Model of Urban Activities From Cellular Data," *IEEE Transactions on Intelligent Transportation Systems* 19, no. 6 (2017), 1682–1696.

47. L. Alexander, S. Jiang, M. Murga, and M. C. González, "Origin–Destination Trips by Purpose and Time of Day Inferred From Mobile Phone Data," *Transportation Research Part C: Emerging Technologies* 58 (2015): 240–250, https://doi.org/10.1016/j.trc.2015.02.018.

48. J. Yin, H. Gu, M. Yu, X. Bao, Y. Xie, and X. Liang, "Synergetic Roles of Dynamic and Cloud Microphysical Processes in Extreme Short-Term Rainfall: A Case-Study," *Quarterly Journal of the Royal Meteorological Society* 148 (2022): 3660–3676, https://doi.org/10.1002/qj.4380.

49. M. C. d. M. Martins, A. N. Rodrigues da Silva, and N. Pinto, "An Indicator-Based Methodology for Assessing Resilience in Urban Mobility," *Transportation Research Part D: Transport and Environment* 77 (2019): 352–363, https://doi.org/10.1016/j.trd.2019.01.004.

50. C. Nan and G. Sansavini, "A Quantitative Method for Assessing Resilience of Interdependent Infrastructures," *Reliability Engineering & System Safety* 157 (2017): 35–53, https://doi.org/10.1016/j.ress.2016.08.013.

51. Y. Liu, X. Wang, C. Song, et al., "Quantifying Human Mobility Resilience to the COVID-19 Pandemic: A Case Study of Beijing, China," *Sustainable Cities and Society* 89 (2023): 104314, https://doi.org/10.1016/j.scs.2022.104314.

52. Y. He, J. Rentschler, P. Avner, J. Gao, X. Yue, and J. Radke. *Mobility and Resilience A Global Assessment of Flood Impacts on Road Transportation Networks* (World Bank, 2022).

53. I. G. Kasmalkar, K. A. Serafin, Y. Miao, et al., "When Floods Hit the Road: Resilience to Flood-Related Traffic Disruption in the San Francisco Bay Area and Beyond," *Science Advances* 6, no. 32 (2020): eaba2423.

54. M. S. G. Adnan, A. Y. M. Abdullah, A. Dewan, and J. W. Hall, "The Effects of Changing Land Use and Flood Hazard on Poverty in Coastal Bangladesh," *Land Use Policy* 99 (2020): 104868, https://doi.org/10.1016/j.landusepol.2020.104868.

55. M. Rahman, C. Ningsheng, G. I. Mahmud, et al., "Flooding and Its Relationship With Land Cover Change, Population Growth, and Road Density," *Geoscience Frontiers* 12 (2021): 101224, https://doi.org/10.1016/j.gsf.2021.101224.

56. S. Talukdar, B. Ghose, Shahfahad, et al., "Flood Susceptibility Modeling in Teesta River Basin, Bangladesh Using Novel Ensembles of Bagging Algorithms," *Stochastic Environmental Research and Risk Assessment* 34 (2020): 2277–2300, https://doi.org/10.1007/s00477-020-01862-5.

57. M. Cools and L. Creemers, "The Dual Role of Weather Forecasts on Changes in Activity-Travel Behavior," *Journal of Transport Geography* 28 (2013): 167–175, https://doi.org/10.1016/j.jtrangeo.2012.11.002.

58. C. Liu, Y. O. Susilo, and A. Karlström, "Weather Variability and Travel Behaviour–What We Know and What We Do Not Know," *Transportation Review* 37 (2017): 715–741, https://doi.org/10.1080/01441647.2017.1293188.

59. G. Forzieri, L. Feyen, S. Russo, et al., "Multi-Hazard Assessment in Europe Under Climate Change," *Climatic Change* 137 (2016): 105–119, https://doi.org/10.1007/s10584-016-1661-x.

60. C. Podesta, N. Coleman, A. Esmalian, F. Yuan, and A. Mostafavi, "Quantifying Community Resilience Based on Fluctuations in Visits to Points-of-Interest Derived From Digital Trace Data," *Journal of the Royal Society, Interface* 18 (2021): 20210158, https://doi.org/10.1098/rsif.2021.0158.

61. D. Sarkar and P. Mondal, "Flood Vulnerability Mapping Using Frequency Ratio (FR) Model: A Case Study on Kulik River Basin, Indo-Bangladesh Barind Region," *Applied Water Science* 10 (2020): 17, https://doi.org/10.1007/s13201-019-1102-x.

62. Z. Kalantari, A. Nickman, S. W. Lyon, B. Olofsson, and L. Folkeson, "A Method for Mapping Flood Hazard Along Roads," *Journal of Environmental Management* 133 (2014): 69–77, https://doi.org/10.1016/j.jenvman.2013.11.032.

63. R. E. Morss, K. J. Mulder, J. K. Lazo, and J. L. Demuth, "How Do People Perceive, Understand, and Anticipate Responding to Flash Flood Risks and Warnings? Results From a Public Survey in Boulder, Colorado, USA," *Journal of Hydrology* 541 (2016): 649–664, https://doi.org/10.1016/j.jhydrol.2015.11.047.

64. C. Shreve, C. Begg, M. Fordham, and A. Müller, "Operationalizing Risk Perception and Preparedness Behavior Research for a Multi-Hazard Context," *Environmental Hazards* 15 (2016): 227–245, https://doi.org/10.1080/17477891.2016.1176887.

65. M. Kuller, K. Schoenholzer, and J. Lienert, "Creating Effective Flood Warnings: A Framework From a Critical Review," *Journal of Hydrology* 602 (2021): 126708, https://doi.org/10.1016/j.jhydrol.2021.126708.

66. J. Li, D. Chen, X. Li, and L. Godding, "Investigating the Association Between Travelers' Individual Characteristics and Their Attitudes Toward Weather Information," *Travel Behaviour and Society* 10 (2018): 53–59, https://doi.org/10.1016/j.tbs.2017.11.001.

67. B. A. Dobson, J. J. Miles-Wilson, I. D. Gilchrist, D. S. Leslie, and T. Wagener, "Effects of Flood Hazard Visualization Format on House Purchasing Decisions," *Urban Water Journal* 15 (2018): 671–681, https://doi.org/10.1080/1573062X.2018.1537370.

68. E. A. Shanahan, A. M. Reinhold, E. D. Raile, et al., "Characters Matter: How Narratives Shape Affective Responses to Risk Communication," *PLoS ONE* 14 (2019): e0225968, https://doi.org/10.1371/journal.pone.0225968.

69. S. H. Potter, P. V. Kreft, P. Milojev, et al., "The Influence of Impact-Based Severe Weather Warnings on Risk Perceptions and Intended Protective Actions," *International Journal of Disaster Risk Reduction* 30 (2018): 34–43, https://doi.org/10.1016/j.ijdrr.2018.03.031.

70. P. Weyrich, A. Scolobig, D. N. Bresch, and A. Patt, "Effects of Impact-Based Warnings and Behavioral Recommendations for Extreme Weather Events," *Weather, Climate, and Society* 10, no. 4 (2018):781–796, https://doi.org/10.1175/WCAS-D-18.

71. D. Chapman, K. Nilsson, A. Larsson, and A. Rizzo, "Climatic Barriers to Soft-Mobility in Winter: Luleå, Sweden as Case Study," *Sustainable Cities and Society* 35 (2017): 574–580, https://doi.org/10.1016/j.scs.2017.09.003.

72. J. Peng and J. Zhang, "Urban Flooding Risk Assessment Based on GIS-Game Theory Combination Weight: A Case Study of Zhengzhou City," *International Journal of Disaster Risk Reduction* 77 (2022): 103080, https://doi.org/10.1016/j.ijdrr.2022.103080.

Appendix

Supplementary Data and Figure

TABLE A1 | Average number of POIs in clusters.

	Cluster 1	Cluster 2	Cluster 3	Cluster 4
Administrative agencies	0.29	9.63	1.89	11.96
Companies and enterprises	1.44	51.72	9.44	55.16
Transportation facilities	2.01	35.01	5.45	44.71
Educational institutions	0.48	11.79	2.58	15.04
Tourist attractions	0.53	0.78	0.32	1.45
Living services	4.42	180.99	20.96	223.4
Residential facilities	0.26	8.85	1.28	10.7
Road density	2.45	7.78	4.82	7.98
River density	18.36	5.22	7.85	5.59

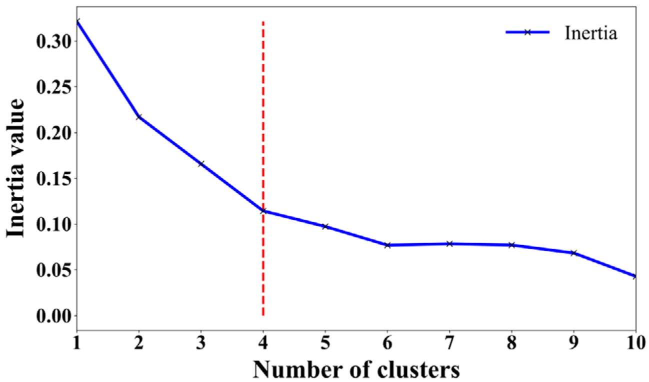

FIGURE A1 | Inertia curve.

TABLE A2 | Hourly based meteorological data on 20 July 2021.

	Hourly warning	Hourly pre-cipitations	Hourly wind
00:00–01:00	0	3.4	7.6
01:00–02:00	0	4.1	8.0
02:00–03:00	0	2.5	5.9
03:00–04:00	0	1.3	4.6
04:00–05:00	0	8.1	3.1
05:00–06:00	0	11.3	5.5
06:00–07:00	1	20.7	6.3
07:00–08:00	0	6.8	5.7
08:00–09:00	0	6.6	7.0
09:00–10:00	1	10.2	9.1
10:00–11:00	0	11.9	7.2
11:00–12:00	0	18.2	8.7
12:00–13:00	1	7.0	7.3
13:00–14:00	1	13.6	6.4
14:00–15:00	0	30.6	6.2
15:00–16:00	0	12.3	8.2
16:00–17:00	1	60.6	14.4
17:00–18:00	0	201.9	12.8
18:00–19:00	0	48.3	10.3
19:00–20:00	0	28.7	6.6
20:00–21:00	0	22.5	5.6
21:00–22:00	1	27.7	3.4
22:00–23:00	0	25.0	5.6
23:00–00:00	0	21.9	4.5

Note: the wind speed is measured in kilometers per hour (km/h), precipitation is measured in millimeters per hour (mm/h). The data is also available on the Wikipedia page with the title " 2021 Henan floods".